Dalton Transactions

Cite this: *Dalton Trans.*, 2011, **40**, 11550

www.rsc.org/dalton

PAPER

Tuning the emissive triplet excited states of platinum(II) Schiff base complexes with pyrene, and application for luminescent oxygen sensing and triplet–triplet-annihilation based upconversions†

Wanhua Wu, Jifu Sun, Shaomin Ji, Wenting Wu, Jianzhang Zhao* and Huimin Guo*

Received 29th May 2011, Accepted 4th August 2011
DOI: 10.1039/c1dt11001b

Pt(II) Schiff base complexes containing pyrene subunits were prepared using the *chemistry-on-complex* approach. This is the first time that supramolecular photochemical approach has been used to tune the photophysical properties of Schiff base Pt(II) complexes, such as emission wavelength and lifetimes. The complexes show intense absorption in the visible region ($\varepsilon = 13100\ M^{-1}\ cm^{-1}$ at 534 nm) and red phosphorescence at room temperature. Notably, much longer triplet excited state lifetimes ($\tau = 21.0\ \mu s$) were observed, compared to the model complexes ($\tau = 4.4\ \mu s$). The extension of triplet excited state lifetimes is attributed to the establishment of equilibrium between the metal-to-ligand charge-transfer (^{3}MLCT) state (coordination centre localized) and the intraligand (^{3}IL) state (pyrene localized), or population of the long-lived ^{3}IL triplet excited state. These assignments were fully rationalized by nanosecond time-resolved difference absorption spectra, 77 K emission spectra and density functional theory calculations. The complexes were used as triplet sensitizers for triplet–triplet-energy-tranfer (TTET) processes, *i.e.* luminescent O_2 sensing and triplet–triplet annihilation (TTA) based upconversion. The O_2 sensitivity (Stern–Volmer quenching constant) of the complexes was quantitatively evaluated in polymer films. The results show that the O_2 sensing sensitivity of the pyrene containing complex ($K_{SV} = 0.04623\ Torr^{-1}$) is 15-fold of the model complex ($K_{SV} = 0.00313\ Torr^{-1}$). Furthermore, significant TTA upconversion (upconversion quantum yield $\Phi_{UC} = 17.7\%$ and the anti-Stokes shift is 0.77 eV) was observed with pyrene containing complexes being used as triplet sensitizers. Our approach to tune the triplet excited states of Pt(II) Schiff base complexes will be useful for the design of phosphorescent transition metal complexes and their applications in light-harvesting, photovoltaics, luminescent O_2 sensing and upconversion, *etc*.

Introduction

Pt(II)/Ir(III) complexes have attracted much attention due to their applications in electroluminescence, photovoltaics, optical limiting, photocatlysis and molecular probes, *etc*.[1–14] These complexes show ^{3}MLCT/^{3}IL mixed triplet excited state, thus the emission is assigned as phosphorescence, featuring large Stoke shifts and long excited state lifetimes.[1,15–26] We have been interested in luminescent transition metal complexes for a while and found that the emission properties of the Pt(II) complexes, such as the emission wavelength and the luminescent lifetimes, can be significantly tuned by introducing organic chromophores.[4–6,27] We explored the applications of these complexes in luminescent oxygen sensing and triplet–triplet annihilation based upconversions.[5,6,28,29]

However, the development of transition metal complexes is facing several challanges, for example, the absorption of the complexes in visible region is weak (the molar extinction coefficient is less than 5000 $M^{-1}\ cm^{-1}$), and the triplet excited state lifetimes are short (usually < 5 μs).[1,2] For the applications of phosphorescent transition metal complexes, intense absorption in visible region and long-lived triplet excited state are highly desired.[30,31] One straightforward approach to acquire intense visible light absorption and long-lived triplet excited states is to attach an organic chromophore to the metal centre. However, it has been shown that the photophysical properties of these dyads are elusive, for example, very often the photophysics of the components collapsed in the dyad, *i.e.* quenching of the phosphorescence, shortening of the triplet excited state lifetime, *etc*, were observed.[31b,31c]

Recently, Pt(II) Schiff base complexes were synthesized and their photophysical properties were studied.[32] The red-shifted UV-vis absorption of these complexes (λ_{abs} = 520 nm) compared to the normal cyclometalated Pt(II) complexes with *C^N* ligand (below

State Key Laboratory of Fine Chemicals, School of Chemical Engineering, Dalian University of Technology, E 208 Western Campus, 2 Ling-Gong Road, Dalian, 116012, P.R. China. E-mail: zhaojzh@dlut.edu.cn, guohm@dlut.edu.cn; Web: http://finechem.dlut.edu.cn/photochem

† Electronic supplementary information (ESI) available: the synthesis and structure characterization data for the Pt(II) complexes; the detailed description of preparation of the sensing films; the details of upconversion, oxygen sensing and calculation information. See DOI: 10.1039/c1dt11001b

450 nm) is particularly interesting.[1] Red-shifted absorption will be beneficial for applications, such as photovoltaics, molecular probes and photocatlysis.[33] Furthermore, these complexes are easy to synthesise and have high phosphorescent quantum yields. However, no applications of these complexes in photophysical processes have been reported. Furthermore, we noticed that the luminescent lifetimes of the typical Pt(II) Schiff base complexes are less than 5 μs.[1,34,35] Longer luminescent lifetime is desired for applications, such as photo-induced charge separation, luminescent oxygen sensing, *etc*.[4,5,36,37] On the other hand, while the tuning of the triplet excited lifetime of the Ru(II) polyimine complexes has been reported,[36,38–40] to the best of our knowledge, however, no study has been carrried out to prolong the triplet excited lifetime of the Pt(II) Schiff base complexes. Thus, much room is left for the study of this kind of novel phosphorescent materials.

Previously we studied Ru(II) polyimine complexes and found that the luminescent lifetime can be extended by 130-fold with the introduction of pyrene subunits to the imine ligand.[36,41] Herein we extend this supramolecular photophysical strategy to tune the excited state lifetimes of Pt(II) Schiff base complexes. We attached pyrene subunits to the Schiff base complexes by C–C bond and C≡C triple bonds, *via* Suzuki cross coupling or Sonogashira coupling reactions. We found that the emissive triplet excited state of the Pt(II) Schiff base complexes can be significantly tuned by pyrene subunits. For example, the triplet excited state lifetime is extended to 21.0 μs. We proposed ^{3}IL triplet excited state was populated in **Pt-6** (Scheme 1). To the best of our knowledge, this is the first time that the excited states of Schiff base Pt(II) complexes are tuned by introducing organic chromophores.

Furthermore, it is for the first time that the long-lived triplet excited states of the Schiff base Pt(II) complexes were used for triplet–triplet-energy-transfer, *i.e.* luminescent oxygen sensing and triplet–triplet annihilation based upconversion. Enhanced luminescence oxygen sensing property (*e.g.* $K_{SV} = 0.04623$ Torr^{-1}) and enhanced upconversion (*e.g.* $\Phi_{UC} = 17.7\%$) were observed for **Pt-5** and **Pt-6**. Our results will be helpful for further exploration of the supramolecular photophysics of the Pt(II) Schiff base complexes and their applications.

Experimental

Materials and reagents

K_2PtCl_4 was purchased from Shandong Boyuan Chemical Co. Ltd. (China), and 1-pyrenylboronic acid is a product of Sigma–Aldrich Co. All the chemicals are analytical purity and were used as received. Solvents were dried and distilled before used for synthesis.

Analytical Measurements

NMR spectra were recorded on a Bruker 400 MHz spectrometer ($CDCl_3$ or DMSO-d_6 as solvents, TMS as standard, $\delta = 0.00$ ppm). High resolution mass spectra (HRMS) were determined on a MALDI micro MX. Fluorescence spectra were measured on a RF5301 fluorospectrometer (Shimadzu) or a CRT 970 spectrofluorometer. The nanosecond time-resolved transient absorption spectra were detected by laser flash photolysis spectrometer (LP920, Edinburgh Instruments, U.K.) and recorded on a Tektronix TDS 3012B oscilloscope. The lifetime values (by monitoring the decay trace of the transients) were obtained with the LP920 software. Luminescence quantum yields of the complexes were measured with Ru(phen)(bpy)$_2$[PF$_6$]$_2$ as the standard ($\Phi = 0.06$ in MeCN). The emission spectra at 77 K was measured with a Oxford Optistat DN™ cryostat (with liquid nitrogen filling) and FS920 fluorospectrometer (Edinburgh Instruments Ltd., U.K.).

Synthesis of Pt-5

Complex **Pt-5** were prepared using *chemistry-on-complex* approach. 1-Pyrenylboronic acid (50.0 mg, 0.20 mmol), complex **2** (119.3 mg, 0.20 mmol), $Pd(PPh_3)_4$ (11.6 mg, 0.01 mmol) and K_2CO_3 (110.4 mg, 0.81 mmol) was charged in a two-necked flask under nitrogen. Degassed DMF (10 mL) was added to the mixture, then the mixture was stirred at 75 °C for 48 h. The majority of solvent was removed and the residue was poured into ice water, the precipitation was collected and washed with water (3 × 30 mL). The crude product was further purified by column chromatography (dichloromethane). Evaporation of solvent from the solution gave a red solid (65.0 mg, 45.8%). ^{1}H NMR (400 MHz, DMSO-d_6): 9.67 (s, 2H), 8.77 (s, 1H), 8.68 (d, 1H, J = 8.7 Hz), 8.47 (d, 1H, J = 8.1 Hz), 8.39–8.29 (m, 4H), 8.26–8.12 (m, 4H), 7.95 (d, 1H, J = 8.1 Hz), 7.84 (d, 1H, J = 6.7 Hz), 7.75 (d, 1H, J = 8.5 Hz), 7.64–7.56 (m, 2H), 7.16 (t, 2H, J = 9.5 Hz), 6.84 (t, 1H, J = 7.5 Hz), 6.76 (t, 1H, J = 7.6 Hz). ^{13}C NMR (100 MHz, d_6-DMSO): 165.1, 152.3, 151.9, 145.4, 140.8, 136.2, 136.0, 131.5, 131.1, 130.3, 128.6, 128.4, 127.9, 127.1, 126.1, 125.7, 125.3, 125.1, 124.6, 124.4, 122.6, 121.7, 118.9, 117.1, 116.8. MALDI-MS: calcd ([$C_{36}H_{22}N_2O_2Pt$]$^+$), m/z = 709.1329, found, m/z = 709.1324. Elemental analysis calculated (%) for $C_{36}H_{22}N_2O_2Pt$: C 60.93, H 3.12, N 3.95; found: C 61.02, H 3.52, N 3.92.

Synthesis of Pt-6

Complex **Pt-6** were prepared using *chemistry-on-complex* approach. Under nitrogen atmosphere, complex **2** (70.0 mg, 0.12 mmol), 1-ethynylpyrene (27.0, 0.12 mmol), $Pd(PPh_3)_2Cl_2$ (8.5 mg, 0.01 mmol), PPh_3 (21.2 mg, 0.08 mmol), and CuI (8.5 mg, 0.05 mmol) were dissolved in DMF (10 mL). The flask was vacuumed and back-filled with argon several times. The mixture was heated to 90 °C for 8 h. The majority of solvent was removed and the residue was poured into ice water, the precipitation was collected and washed with water (3 × 30 mL). The crude product was further purified by washing with CH_2Cl_2 several times, dark red solid was obtained (40 mg, 45.5%). ^{1}H NMR (400 MHz, DMSO-d_6): 9.72 (s, 1H), 9.61 (s, 1H), 8.90 (s, 1H), 8.76 (d, 1H, J = 8.7 Hz), 8.60 (d, 1H, J = 8.1 Hz), 8.46–8.25 (m, 7H), 8.17 (t, 1H, J = 8.1 Hz), 7.97–7.88 (m, 3H), 7.62 (t, 2H, J = 6.7 Hz), 7.17 (d, 2H, J = 8.5 Hz), 6.86–6.81 (m, 2H). ^{13}C NMR (100 MHz, d_6-DMSO): 164.7, 152.0, 151.6, 144.8, 135.8, 135.7, 131.3, 130.8, 129.7, 129.1, 128.7, 127.2, 126.9, 126.1, 125.0, 121.3, 119.6, 117.1, 116.5, 116.5, 94.3, 90.1. MALDI-MS: calcd ([$C_{38}H_{22}N_2O_2Pt$]$^+$), m/z = 733.1329, found, m/z = 733.1336. Elemental analysis calculated (%) for $C_{38}H_{22}N_2O_2Pt \cdot 2.5$ (DMSO): C 55.59, H 4.01, N 3.02; found: C 55.41, H 3.41, N 3.05 (the sample was recovered from the NMR measurement).

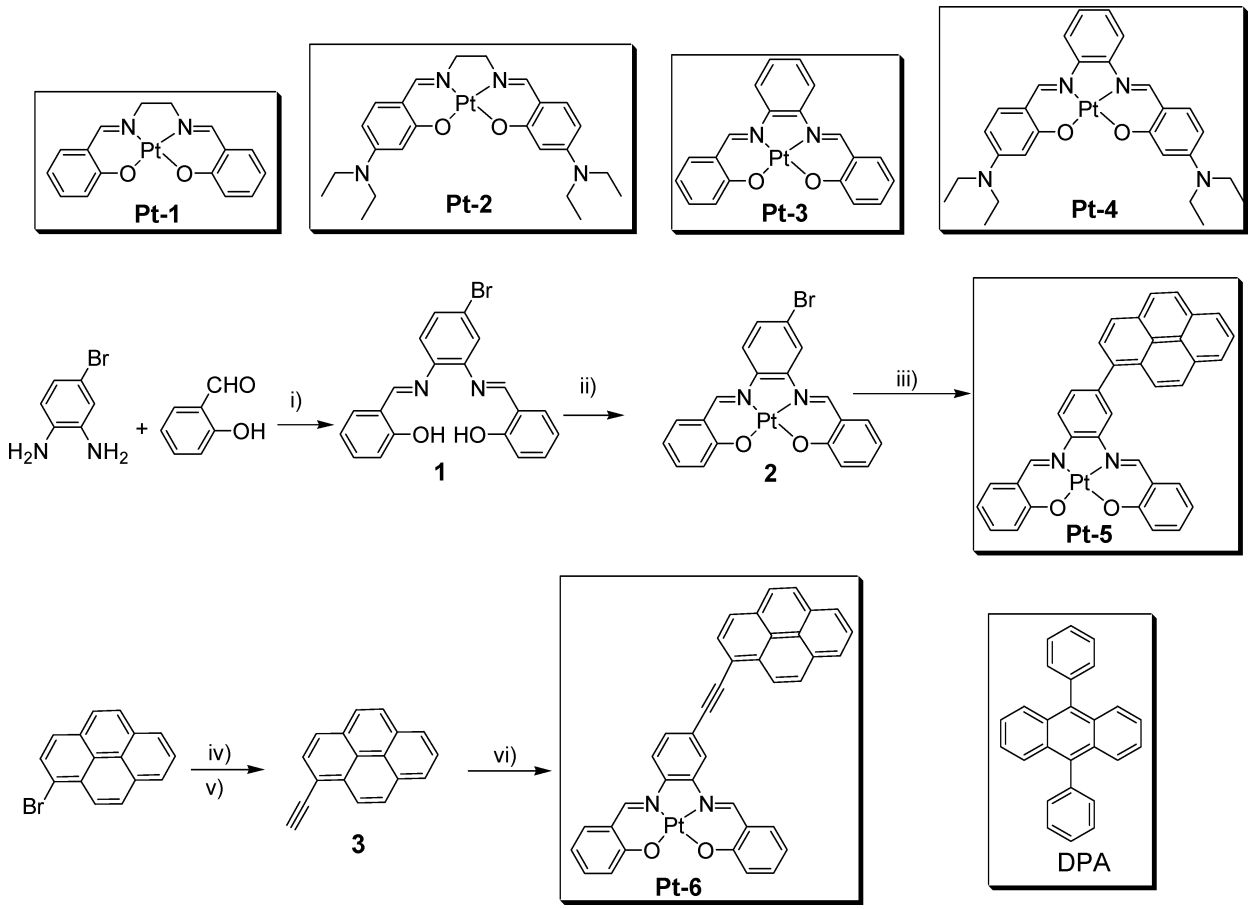

Scheme 1 Synthesis of the complexes **Pt-5** and **Pt-6**. The known complexes **Pt-1**, **Pt-2**, **Pt-3** and **Pt-4** were used in photophysical studies as model complexes. i) Ethanol, r.t.; ii) K_2CO_3, K_2PtCl_4, DMSO; iii) 1-Pyrenylboronic acid, $Pd(PPh_3)_4$, K_2CO_3, iv) Trimethylsilylacetylene, $Pd(PPh_3)_4$, CuI, TEA, reflux, 8 h; v) K_2CO_3, MeOH; vi) **2**, $Pd(PPh_3)_4$, CuI, TEA, DMF.

Computational Methods

The geometry optimizations were calculated using B3LYP functional with the 6-31G(d)/LanL2DZ basis set with density functional theory (DFT). The excitation energy was calculated using the time-dependent DFT (TDDFT) method based on the optimized singlet ground state geometry. The spin-density of the triplet state was calculated with the energy minimized triplet state geometries. All calculations were performed using Gaussian 09 W (Gaussian, Inc.).[42]

Upconversions

Diode pumped solid state laser was used as the excitation source for the upconversions. The samples were purged with N_2 or Ar for 15 min before measurement. The upconversion quantum yields were determined with the phosphorescence of $Ru(dmb)_3[PF_6]_2$ as the quantum yield standard (Φ = 0.074 in MeCN) and the quantum yields were calculated using eqn (1),

$$\Phi_{unk} = 2\Phi_{std}\left(\frac{A_{std}}{A_{unk}}\right)\left(\frac{I_{unk}}{I_{std}}\right)\left(\frac{\eta_{unk}}{\eta_{std}}\right)^2 \quad (1)$$

where Φ_{unk}, A_{unk}, I_{unk} and η_{unk} represent the quantum yield, absorbance, integrated photoluminescence intensity and the refractive index of the samples, respectively (unk means unknown).[43] The photography of the upconversion were taken with Samsung NV 5 digital camera. The exposure times are the default values of the camera.

Results and Discussions

Design and Synthesis of the Complexes

The reported complexes **Pt-1–Pt-4** were prepared for comparison in the photophysical studies (Scheme 1). Complexes **Pt-2** and **Pt-4** have significant intramolecular charge transfer (ICT) effects due to the diethylamino group on the salicaldehyde moiety. In order to introduce the pyrene units, we used 4-bromo-1,2-benzenediamine as the precursor. Then *chemistry-on-complex* approach was used to attach pyrene or pyreneethynylene subunit on the complexes by Sonogashira or Suzuki coupling reaction (Scheme 1).[36,41] To the best of our knowledge, *chemistry-on-complexes* synthetic methodology was rarely used for preparation of the Schiff base Pt(II) complexes. All the complexes were obtained with good yields.

UV-vis absorption spectra of the complexes

The UV-vis absorptions of the complexes were studied (Fig. 1). **Pt-3** shows more red-shifted absorption (521 nm) than **Pt-1** (419 nm).

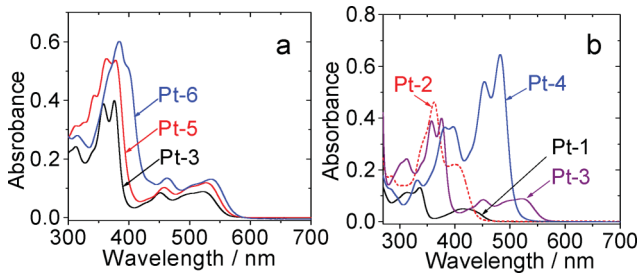

Fig. 1 UV-vis absorption spectra of **Pt-3**, **Pt-5** and **Pt-6** in MeCN (1.0×10^{-5} M), (b) UV-vis absorption spectra of **Pt-1**, **Pt-2**, **Pt-3** and **Pt-4** in MeCN (1.0×10^{-5} M). 20 °C.

Interestingly, the UV-vis absorption of **Pt-2** and **Pt-4** show blue-shifting with the introduction of electron-donating diethylamino group, compared to **Pt-1** and **Pt-3**. This is probably due to the attachment of electron-donating moiety on the moiety where LUMO is localized (see ESI†).[1,32] The intense absorption band at the red end of the spectra is due to the ^{1}MLCT/^{1}IL transitions, usually, the absorption of ^{1}MLCT of the Pt(II) complexes is very weak and at much shorter wavelength. Previously, we increased the absorption wavelength by introducing organic chromophores with intense absorption in visible range.[5,6] The absorption in the blue range is due to the π–π* transition of the ligands. With introduction of pyrene, the absorptions of **Pt-5** and **Pt-6** show red-shifted absorption bands.

The UV-vis absorption of **Pt-6** in different solvents was studied (see ESI†) and the results show that blue-shifted absorption was observed in polar solvents relative to that in non-polar solvents. This result indicates that the dipole moment of the Frank Condon excited state is smaller than that of ground state.[32] Same results were found for other complexes (see ESI†).

Emission spectra of the complexes at room temperature

The emission of the complexes was studied and room temperature (RT) phosphorescence was observed (Fig. 2). With extension of the π-conjugation (**Pt-1** *vs.* **Pt-3**), the emission is red-shifted by 60 nm. Interestingly, with introduction of the electron-donating diethylamino group, a hypsochromic shift was observed for the emission of the complexes. For example, emission at 600 nm was observed for **Pt-4**, *vs.* the emission at 614 nm for **Pt-3**. **Pt-5** shows an emission band which is similar to **Pt-3**. For **Pt-6**, however, red-shifted emission at 667 nm was observed. Furthermore, the vibrational structure of the emission band of **Pt-6** is different from those of the other complexes. Thus we propose that the emissive state of **Pt-6** is different from **Pt-3**, most probably the ^{3}IL triplet excited state (localized on the ethynylate pyrene subunit) is populated. Previously we observed similar ^{3}IL emission for Ru(II) complex containing ethynylated pyrene ligand.[36]

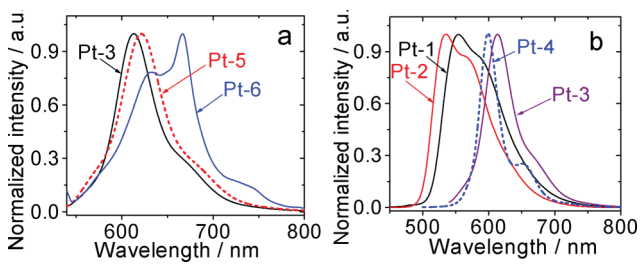

Fig. 2 Normalized emission of **Pt-3**, **Pt-5** and **Pt-6** in MeCN solution (1.0×10^{-5} M). (b) Normalized emission of **Pt-1**, **Pt-2**, **Pt-3** and **Pt-4** in MeCN solution (1.0×10^{-5} M). 20 °C.

Emission spectra at 77 K

In order to study the emissive triplet excited states of the complexes, the emission spectra at 77 K were studied (Fig. 3). It is known that thermally induced Stokes shift (ΔE_S) is an indication of the ^{3}IL or ^{3}MLCT feature of the emissive triplet excited state.[44,45] For **Pt-3**, the emission at 77 K is more structured than that at RT. The thermally induced Stokes shift is 584 cm^{-1}. Thus we propose that ^{3}MLCT is the major component of the emissive triplet excited state of **Pt-3**. For **Pt-5** and **Pt-6**, however, much smaller thermally induced Stokes shifts were observed, ΔE_S = 211 cm^{-1} and 90 cm^{-1} for **Pt-5** and **Pt-6**, respectively. Thus we propose that ^{3}IL is the major component of the emissive triplet excited states of **Pt-5** and **Pt-6**. This conclusion is supported by the time-resolved transient difference absorption spectra and the DFT calculations.

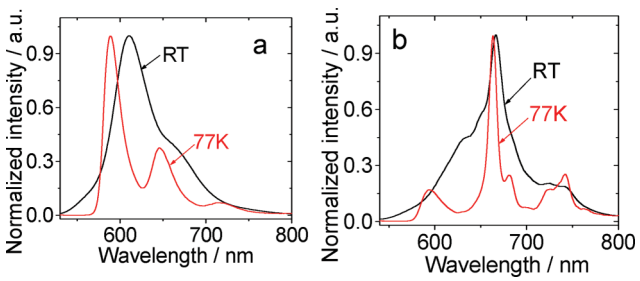

Fig. 3 Emission spectra of **Pt-3**, and **Pt-6** in ethanol-methanol (4 : 1, v/v) glass at 77 K and solution at RT (298 K). (a) **Pt-3**, λex = 520 nm; (b) **Pt-6**, λex = 530 nm.

Nanosecond time-resolved transient difference absorption

The nanosecond time-resolved difference absorption spectra were studied (Fig. 4). For the parent complex **Pt-3**, a significant bleaching band at 450 nm was observed upon pulsed laser excitation, which is due to the depletion of the ground state of **Pt-3** upon photoexcitation. Transient absorption bands in the 500 nm–600 nm range were observed. The triplet excited state lifetime is 4.4 μs, which is in good agreement with the result obtained by the luminescence method. Thus we conclude that the triplet excited state we observed is the emissive excited state, which leads to the RT phosphorescence of **Pt-3**. For **Pt-5**, bleaching at 450 nm

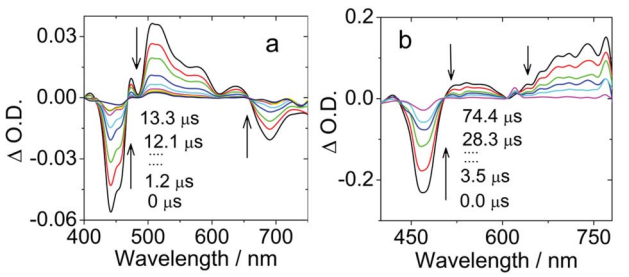

Fig. 4 Nanosecond time-resolved transient difference absorption spectra of (a) **Pt-3** and (b) **Pt-6** after pulsed excitation (λ_{ex} = 532 nm). In deaerated MeCN. 20 °C.

Table 1 Photophysical parameters of the Pt(II) Schiff base complexes

			Emission Properties				
Compounds	λ_{abs} (nm)[a]	ε[b]	λ_{em} (RT)[a]	λ_{em} (77 K)[c]	Φ[d]	I_0/I_{100}[e]	τ (10^{-5}mol L^{-1}) (μs)[f]
Pt-1	336, 419	1.31, 0.487	554	520, 564, 612	0.19	212.5	3.5 (lit. 3.4)
Pt-2	363, 402	4.61, 2.2	535	504, 547, 598	0.13	301.5	3.1
Pt-3	358, 376, 450, 521	3.90, 4.01,0.85, 0.89	614	589, 646, 716	0.23	194	4.4
Pt-4	454, 482	5.41, 6.5	600	589, 648, 716	0.22	649	6.1
Pt-5	363, 378, 459, 527	5.43, 5.37, 1.03, 1.2	621	612, 675, 753	0.14	1256	13.4[g]
Pt-6	384, 462, 534	6.01, 1.35, 1.31	632, 667	593, 663, 742	0.034	423	21.0[g]

[a] Result of compounds in MeCN solution (1.0×10^{-5} mol dm^{-3}). [b] Molar extinction coefficient at the absorption maxima. ε:10^4 M^{-1} cm^{-1}. [c] Result in ethanol-methanol (4 : 1, *v*/*v*) glass at 77 K. [d] Result of deaerated solution, with complex Ru(phen)(bpy)$_2$ (Φ = 0.06 in MeCN) as the standard. [e] The emission intensity ratio of the complexes under nitrogen and oxygen atmosphere, I_0 stands for the emission intensity in N_2 and I_{100} stands for the emission in O_2 atmosphere. [f] Luminescent lifetimes. [g] Lifetimes measured by nanosecond time-resolved transient absorptions, 1.0×10^{-5} M in MeCN. In deaerated solution.

was observed (see ESI†), which is due to the depletion of the ground state of the complex upon photoexcitation. Furthermore, significant transient absorption in the 600 nm–800 nm region was found. Similar transients were observed for **Pt-6** (Fig. 4(b)). The significant absorption profile in the 600 nm–800 nm region is similar to that for pyrene-containing Pt(II) complexes, reported by us previously.[27–37] Thus we conclude that ^{3}IL component is significant for the emissive excited state of **Pt-5** and **Pt-6**.

The photophysical parameters of the complexes are compiled in Table 1. The highly phosphorescent quantum yield is still present in **Pt-5** (Φ = 14%). For **Pt-6**, however, the quantum yield is much lower. Furthermore, we observed that the luminescent lifetimes of **Pt-5** and **Pt-6** (τ = 21.0 μs) are much longer than that of the model complex **Pt-3** (τ = 4.4 μs), and much longer than the dbbpy Pt(II) complexes, *e.g.* 8-fold longer than a dbbpy Pt(II) complexes we recently reported.[5] We propose that the extended lifetime of **Pt-5** is due to the equilibrium between the ^{3}MLCT state (coordination centre localized) and the ^{3}IL state (pyrene localized).[36,38,39,40]

For **Pt-6**, the long lifetime is due to the ^{3}IL state.[36] The high phosphorescence quantum yield and the long triplet excited state lifetime are ideal for applications such as photo-induced charge separation, triplet–triplet-energy-transfer (luminescent oxygen sensing and TTA upconversion), *etc*.

DFT calculations

DFT calculations are important for study of fluorescent molecular probes, with which luminophores can be prepared with predetermined photophysical properties.[4,17–19,21,46,47] Recently Zn^{2+} probes were studied by DFT calculations.[48] Previously we studied the fluorescence response of thiol probes, boronic acid molecular probes, and predicted the photophysics of phosphorescent transition metal complexes with DFT calculations.[3–6,36,46,47,49] Herein we carried out DFT and time-dependent DFT (TDDFT) calculations to rationalize the photophysical properties of the Pt(II) Schiff base complexes.

In order to study the UV-vis absorption and the phosphorescence of the complexes, density functional theory (DFT) calculations were carried out. For **Pt-3**, the optimized ground state geometry is coplanar. The frontier molecular orbitals are presented in Fig. 5. HOMO is distributed on the Pt(II) metal and the π-conjugation framework of the complex. Pt(II) is not involved in the LUMO. The predicted UV-vis absorption at 526 nm is in good agreement with the experimentally observed absorption at 521 nm (Fig. 1 and Table 1). HOMO→LUMO is involved in the $S_0 \rightarrow S_1$ transition. Thus the absorption band of **Pt-3** at 521 nm (Fig. 1) can be assigned as ^{1}MLCT/^{1}IL transition.

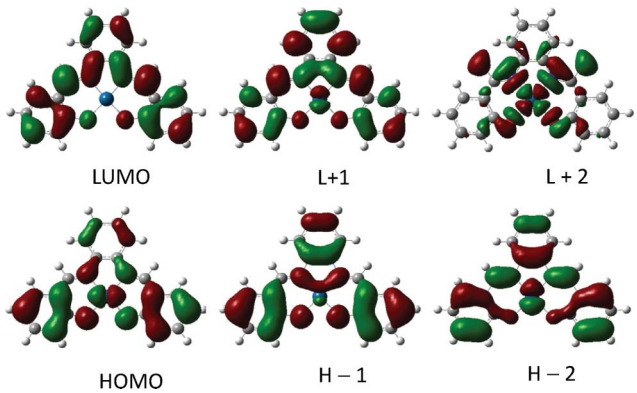

Fig. 5 Frontier molecular orbitals of **Pt-3**. H stands for HOMO and L stands for LUMO. Calculated by DFT at the B3LYP/6-31G((d)/LanL2DZ level using Gaussian 09W.[42]

In order to study the emission of **Pt-3**, the energy gap between the S_0 state and the T_1 excited states were calculated by TDDFT (Table 2). The calculated emission band at 660 nm is in good agreement with the experimental results (Fig. 2). Based on the distributions of the frontier MOs of the transition, the emissive excited state of **Pt-3** can be assigned as ^{3}MLCT/^{3}IL mixed feature.

For the dyad **Pt-5**, the pyrene moiety is not in full π-conjugation with the Schiff base-Pt(II) coordination center. The optimized geometry shows that the pyrene moiety tilted by 53.9° to the Schiff base-Pt(II) coordination plane (Fig. 6). The calculated UV-vis absorption at 533 nm is in good agreement with the experimentally observed absorption band at 527 nm (Fig. 1). Based on the TDDFT calculations, HOMO→LUMO is involved in the $S_0 \rightarrow S_1$ transition (See ESI†). The distributions of HOMO and LUMO demonstrated that the $S_0 \rightarrow S_1$ transition is ^{1}MLCT/^{1}IL (Fig. 6). Pyrene moiety does not contribute significnatly to the $S_0 \rightarrow S_1$ transition. The phosphorescence of **Pt-5** was studied by TDDFT calculations (See ESI† for the details of the transitions). The calculated $S_0 \rightarrow T_1$ energy gap (*i.e.* the emission wavelength) is in good agreement with the experimental results.

The geometry of **Pt-6** was also optimized by DFT calculations. The pyrene moiety takes a coplanar geometry toward the Pt(II)

Table 2 Electronic excitation energies (eV) and corresponding oscillator Strengths (*f*), main configurations and CI coefficients of the low-lying electronically excited states of **Pt-3**, calculated by TDDFT//B3LYP/6-31G(d)/lanl2dz, based on the optimized ground state geometries

		TDDFT//B3LYP/6-31G(d)				
	Electronic transition	Energy[a]	*f*[b]	Composition[c]	CI[d]	character
Singlet	$S_0 \rightarrow S_1$	2.36 eV 526 nm	0.0554	HOMO → LUMO	0.6708	MLCT
	$S_0 \rightarrow S_2$	2.78 eV 446 nm	0.0320	HOMO-1→LUMO	0.6710	ILCT
	$S_0 \rightarrow S_5$	3.41 eV 364 nm	0.4982	HOMO-2→LUMO	0.6519	MLCT
	$S_0 \rightarrow S_6$	3.43 eV 362 nm	0.1728	HOMO-4→LUMO	0.1604	MLCT
				HOMO-1→LUMO+1	0.6467	ILCT
Triplet	$S_0 \rightarrow T_1$	1.88 eV 660 nm	0.0000[e]	HOMO-1→ LUMO+1	0.2348	ILCT
				HOMO → LUMO	0.7130	MLCT
	$S_0 \rightarrow T_2$	2.06 eV 601 nm	0.0000[e]	HOMO-1→ LUMO	0.5907	ILCT
				HOMO→ LUMO+1	0.4735	MLCT

[a] Only the selected low-lying excited states are presented. [b] oscillator strength. [c] Only the main configurations are presented. [d] The CI (configuration interaction) coefficients are in absolute values. [e] No spin-orbital coupling effect was considered, thus the *f* values are zero

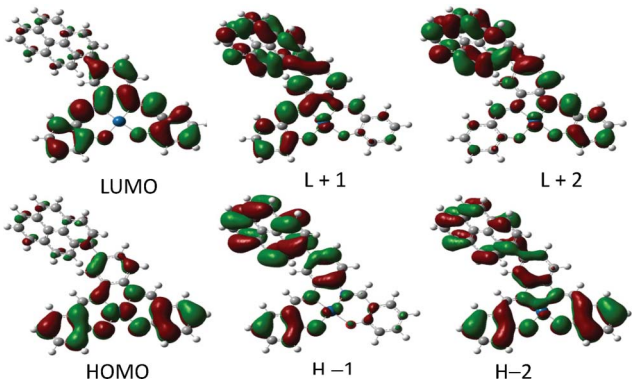

Fig. 6 Frontier molecular orbitals of **Pt-5**. H stands for HOMO and L stands for LUMO. Calculated by DFT at the B3LYP/6-31G((d)/LanL2DZ level using Gaussian 09W.[42]

coordination plane of the complex. Thus the pyrene moiety is in full π-conjugation with the coordination center. We found the frontier MOs are distributed on the coordination and the pyrene moiety, which is different from that of **Pt-5** (Fig. 7). The calculated UV-vis absorption maxima of **Pt-6** are located at 548 nm, 483 nm and 423 nm, which are in good agreement with the experimental results of 534 nm, 462 nm and 384 nm (Fig. 1).

For the T_1 excited state (Table 3), HOMO →LUMO and HOMO-1→LUMO+1 are the main components of the $S_0 \rightarrow T_1$ transition, thus the major feature of the T_1 state is ^{3}IL, which is localized on the pyrene-acetylide conjugated ligand.

The calculated $S_0 \rightarrow T_1$ energy gap (714 nm) is in good agreement with the experimentally observed 667 nm (note there is an emission shoulder at 720 nm, Fig. 2).

The involvement of the pyrene moiety in the triplet excited state manifold of **Pt-5** and **Pt-6** were also indicated by the spin density analysis of the triplet state of the complexes (Fig. 8). For the model complex **Pt-3**, the spin density is distributed on the Schiff base ligand, as well as on the Pt(II) center. For **Pt-5** and **Pt-6**, however, the contributions of pyrene moiety to spin density are significant, which rationalize the long-lived T_1 excited state of the complexes. Based on the steady state spectroscopy, we propose that for **Pt-5**, the ^{3}MLCT/^{3}IL equilibrium and for **Pt-6**, the population of the ^{3}IL state, are responsible for the prolonged T_1 state lifetimes, respectively.

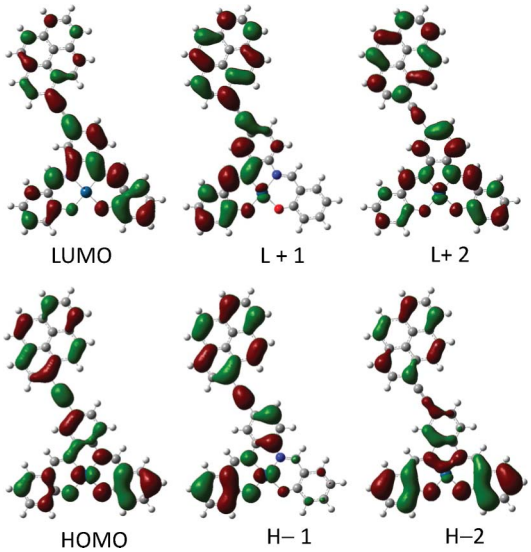

Fig. 7 Frontier molecular orbitals of **Pt-6**. H stands for HOMO and L stands for LUMO. Calculated by DFT at the B3LYP/6-31G((d)/LanL2DZ level using Gaussian 09W.[42]

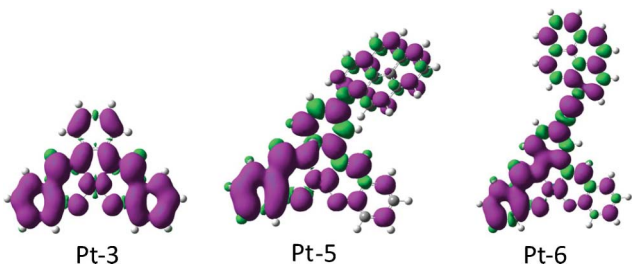

Fig. 8 Spin density surface of **Pt-3**, **Pt-5** and **Pt-6** at the optimized triplet state geometry. Calculated at B3LYP/6-31G/LANL2DZ level with Gaussian 09W.[42]

Application of the Efficient Triplet–triplet energy tranfer: Enhanced Luminescent O_2 sensing

Previously we proposed that the long-lived ^{3}IL excited state can be used for efficient triplet–triplet energy transfer, such as luminescent oxygen sensing,[36] because the phosphorescence of transition metal complexes can be significantly quenched by O_2.[50] Since the current Pt(II) Schiff base complexes show absorption in visible region and

Table 3 Electronic excitation energies (eV) and corresponding oscillator Strengths (*f*), main configurations and CI coefficients of the low-lying electronically excited states of complex **Pt-6**, calculated by TDDFT//B3LYP/6-31G(d)/lanl2dz, based on the optimized ground state geometries

		TDDFT//B3LYP/6-31G(d)				
	Electronic transition	Energy (eV)[a]	*f*[b]	Composition[c]	CI[d]	character
Singlet	$S_0 \rightarrow S_1$	2.26 eV 548 nm	0.2694	HOMO-1 → LUMO	0.2303	MLCT, ILCT
				HOMO→ LUMO	0.6171	MLCT
				HOMO→ LUMO+1	0.1276	MLCT, ILCT
	$S_0 \rightarrow S_2$	2.57 eV 483 nm	0.2923	HOMO-2→LUMO	0.2021	ILCT
				HOMO-1→LUMO	0.6024	MLCT, ILCT
				HOMO→LUMO	0.2039	MLCT
	$S_0 \rightarrow S_5$	2.93 eV 423 nm	0.7691	HOMO-1→LUMO+1	0.6147	MLCT, ILCT
				HOMO-1→LUMO+2	0.1307	ILCT
				HOMO→LUMO+1	0.2029	MLCT, ILCT
	$S_0 \rightarrow S_9$	3.30 eV 376 nm	0.2919	HOMO-3→LUMO	0.6163	MLCT
				HOMO-2→LUMO+1	0.2368	ILCT
				HOMO-1→LUMO+2	0.1066	ILCT
Triplet	$S_0 \rightarrow T_1$	1.74 eV 714 nm	0.0000[e]	HOMO-2 → LUMO+1	0.1333	ILCT
				HOMO-2 → LUMO+2	0.1734	ILCT
				HOMO-1 → LUMO	0.2248	MLCT, ILCT
				HOMO-1 → LUMO+1	0.2711	MLCT, ILCT
				HOMO-1 → LUMO+2	0.1822	ILCT
				HOMO → LUMO	0.5874	MLCT
				HOMO → LUMO+1	0.2240	MLCT, ILCT
	$S_0 \rightarrow T_2$	1.87 eV 665 nm	0.0000[e]	HOMO-2→LUMO	0.1157	ILCT
				HOMO-2→LUMO+1	0.1919	ILCT
				HOMO-1→LUMO	0.4777	MLCT, ILCT
				HOMO-1→LUMO+2	0.1665	ILCT
				HOMO→LUMO	0.3414	MLCT
				HOMO→LUMO+1	0.3497	MLCT, ILCT
				HOMO→LUMO+2	0.1415	MLCT

[a] Only the selected low-lying excited states are presented. [b] Oscillator strength. [c] Only the main configurations are presented. [d] The CI coefficients are in absolute values. [e] No spin-orbital coupling effect was considered, thus the *f* values are zero.

long lived triplet excited state, thus these complexes are used for luminescent O_2 sensing.

The emission of the complexes was significantly quenched in air relative to that under inert atmosphere. Thus, we anticipate efficient triplet–triplet energy transfer between the triplet excited states of the complexes and the O_2 molecule (which is at triplet state).[50,51] Furthermore, we found that the emission of the pyrene-containing **Pt-5** and **Pt-6** was completely quenched in air, but the emission of the model complex **Pt-3** is detectable in air, thus we anticipate longer luminescent lifetimes for **Pt-5** and **Pt-6** compared to **Pt-3**. In later sections we explore the application of the complexes in triplet–triplet-energy-transfer processes, such as the luminescent oxygen sensing and the triplet–triplet annihilation based upconversion.

In order to quantitatively evaluate the O_2 sensing properties, sensing films, prepared by distribution of the complexes in polymer film, were used together with flow cell which is coupled to spectrofluorometer *via* optical fibers.[4,36,37,41,43,52–55] Thus we can continuously monitor the change of phosphorescence intensity of the sensing films *vs.* the variation of O_2 partial pressure in the gas sample (Fig. 9).

Two types of sensing experiments were carried out, one is to monitor the phosphorescence response of the sensing films by switching between N_2 and O_2. Thus the response time ($t_{95}\downarrow$) and the recovery time ($t_{95}\uparrow$) of the films can be studied. Moreover, the phosphorescence response of the films toward small steps of O_2 partial pressure variation were also monitored, the data can be used to derive the Stern–Volmer quenching constant of the sensing film.

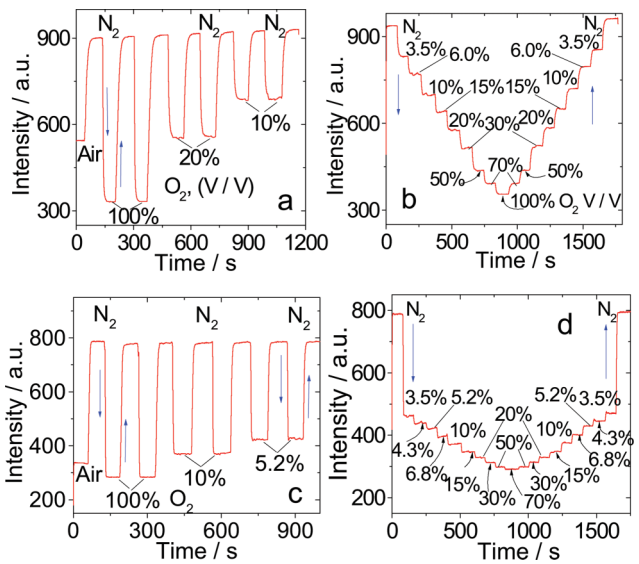

Fig. 9 Phosphorescence intensity response of the complexes to step variations of O_2 concentration levels. (a) and (c) emission change of **Pt-3** and **Pt-6** film *vs.* O_2/N_2 saturation switch, (b) and (d) dynamic response of the **Pt-3** and **Pt-6** film *vs.* small steps of variation of O_2 partial pressure. **Pt-3**: λ_{ex} = 526 nm, λ_{em} = 609 nm; **Pt-6**: λ_{ex} = 530 nm, λ_{em} = 667 nm. 20 °C.

Fast response time and recovery were found for the sensing films. For example, the response time of the **Pt-6** is 6.4 s and the recovery time is 14.6 s, similar kinetics were found for the other complexes. Fast response and recovery were usually found for the O_2 sensing

materials with porous materials, such as molecular sieves. The preparation of our O_2 sensing films is dissolution-casting, which is straightforward for practical applications.

The phosphorescence emission of **Pt-3** is sensitive to O_2. For example, by increasing the O_2 partial pressure from 0.0% to 3.5%, the phosphorescence emission was quenched by 18.3%. The dynamic range is up to 100% O_2 (mixed gas with N_2, *v*/*v*). For **Pt-5**, higher O_2 sensitivity was observed. For example, the phosphorescence is more significantly quenched with 3.5% O_2.

Higher O_2 sensitivity was observed for **Pt-6** (Fig. 9 and ESI† for other complexes). It should be pointed out that the photostability of the sensing films is excellent, the emission intensity of the sensing films are fully reversible after long time of continuous irradiation, which is better than the PtOEP O_2 sensing materials.[52,56]

For the heterogeneous O_2 sensing, usually two-site model was used.[50] In this model, the dye molecules are considered as two different portions, which are defined as f_1 and f_2, respectively ($f_1 + f_2 = 1$). Each portion show different quenching constants (K_{SV1} and K_{SV2}, eqn (2)).

$$\frac{I_0}{I} = \frac{1}{\frac{f_1}{1+K_{SV1}p_{O_2}} + \frac{f_2}{1+K_{SV2}p_{O_2}}} \quad (2)$$

The fitting result is presented in Fig. 10. **Pt-5** and **Pt-6** gave faster responses than the other complexes. Numeric fitting give the Stern–Volmer quenching constants (Table 4). We can see that the oxygen sensitivity of **Pt-6** is 9.1-fold of that of the model complex **Pt-3**, and 4-fold of the complexes reported by us recently.[5] Furthermore, the O_2 sensitivity of **Pt-6** is 13.2-fold of a recently reported cyclometallated Ir(III) complex (τ = 4.3 μs in inert atmosphere) for O_2 sensing purpose.[57]

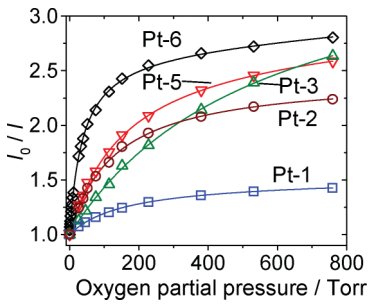

Fig. 10 Fitting of the O_2 sensing property of the IMPEK-C films of the complexes based on the two site model (eqn (2)).

Application of the complexes for efficient triplet–triplet-energy-transfer: enhanced triplet–triplet annihilation based low-power upconversion

Transition metal complexes with intense absorption in the visible region and long-lived triplet excited states can be used for applications other than luminescent O_2 sensing. Herein, we set out to employ the long-lived triplet excited states of **Pt-5** and **Pt-6** in the newly developed triplet–triplet annihilation (TTA) based upconversion.[5,6,28,29,58–65]

TTA upconversion is a promising upconversion scheme due to it requiring low excitation power (sunlight is sufficient), and the readily changeable excitation/emission wavelength. However, the current development of TTA based upconversion is facing some challenges. For example, the triplet sensitizers are limited to Ru(II) and Pt(II) porphyrin complexes.[28,43,58–60] It is difficult to tune the T_1 energy levels of these complexes.

Similar to the luminescent O_2 sensing studies, we propose that complexes with longer triplet excited state lifetimes will be more efficient to sensitize a TTA based upconversion.[5,6,28,29] However, no studies have been carried out to investigate the relationship between the lifetime and the efficiency of the upconversion.

Previously we have demonstrated that Ru(II) polyimine complexes with ^{3}IL state are much more efficient to sensitize TTA based upconversion.[28] However, the Ru(II) complexes we used previously still suffer from poor absorption in the visible range. The Pt(II) Schiff base complexes (Scheme 1) show more intense absorption in the visible range. For example, the molar extinction coefficient of **Pt-6** is 1.3×10^4 $M^{-1}cm^{-1}$ at 532 nm, *vs.* 1.0×10^3 for $[Ru(dmb)_3]^{2+}$ or $Ru(Phen\text{-}pyrene)(bpy)_2$.[36] Furthermore, the lifetime of the typical ^{3}MLCT state of the normal Ru(II) polyimine complexes is less than 1 μs (for $[Ru(dmb)_3]^{2+}$, τ = 0.84 μs in CH_3CN and 0.33 μs in H_2O). Therefore, we expected more efficient upconversion with **Pt-5** and **Pt-6**. The long lifetimes of the T_1 states of **Pt-5** and **Pt-6** will also improve the upconversion efficiency.

Since the complexes show intense absorption in the visible range, which is better than the normal Ru(II) polyimine complexes and the *C^N* cyclometalated Pt(II) complexes,[1,5] thus we used a 532 nm laser to excite the complexes (Fig. 11). The complexes demonstrated different emission intensities, which are roughly in line with the luminescent quantum yields (Table 1). Notably **Pt-6** emits weakly with 532 nm excitation. **Pt-3** gives the strongest emission (*ca.* 4 times that of **Pt-6**). **Pt-5** gives emission similar to **Pt-3**. With addition of 9,10-diphenylanthracene (DPA) into the complex solution, the phosphorescence of the complexes was

Table 4 Parameters of O_2 sensing films of complexes with IMPEK-C cardo poly(aryl ether ketone)[4] as supporting matrix (fitting result of the two site model)

	f_1[a]	f_2[a]	K_{SV1}[b]	K_{SV2}[b]	r^2[c]	K_{SV}^{app}[d]	pO_2[e]/Torr
Pt-1	0.3328	0.6672	0.0094	0.0000	0.9998	0.00313	106.4
Pt-2	0.5926	0.4074	0.0188	0.0000	0.9993	0.0111	53.2
Pt-3	0.7381	0.2619	0.0069	0.0000	0.9996	0.00509	144.9
Pt-4	0.9337	0.0663	0.0202	0.0001	0.9999	0.01887	49.5
Pt-5	0.6451	0.3549	0.0179	0.0000	0.9996	0.01155	55.9
Pt-6	0.6336	0.3664	0.0729	0.0001	0.9993	0.04623	13.7

[a] The ratio of the two portions of the dyes. [b] The quenching constants of the two portions. [c] The determination coefficients. [d] Weighted quenching constant, $K_{SV}^{app} = f_1 \times K_{SV1} + f_2 \times K_{SV2}$. [e] The oxygen partial pressure at which the initial emission intensity of film is quenched by 50%, and can be calculated as $1/K_{SV}$.

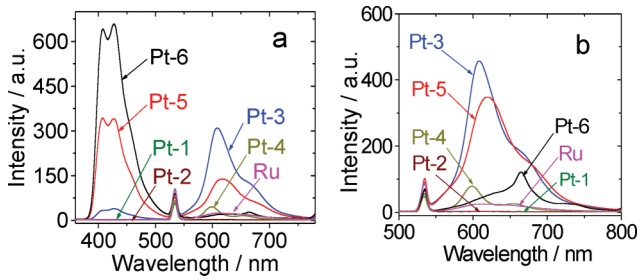

Fig. 11 Upconversion with the complexes as sensitizers and DPA as acceptor. (a) Upconverted DPA emission intensity and residual photoluminescence of the sensitizers following excitation at 532 nm. In deaerated CH_3CN. *c* [complexes] = 2.0×10^{-6} M, *c* [DPA] = 1.1×10^{-5} M. (b) Phosphorescence intensity profiles of complexes without DPA under the same conditions. 20 °C.

quenched to different extents. For example, the emission of **Pt-3** was quenched slightly (by 32%). For **Pt-5**, however, the quenching is more significant (by 61%). At the same time as the quenching of phosphorescence by DPA, upconverted blue fluorescence of DPA at 400 nm–500 nm was observed. Excitation of the complexes or DPA alone by 532 nm laser did not produce the blue fluoresecence. This control experiment verified the upconverted fluorescence of DPA.

Interestingly, we observed more efficient upconversion for **Pt-5** and **Pt-6** compared to **Pt-3**. The Ru(II) polyimine complex, $[Ru(dmb)_3][PF_6]_2$, was also studied and no upconversion was observed under the same experimental conditions (such as the concentration of DPA, please note that the concentration of DPA here is much lower than the literature value and the values we have reported),[5,6,28,29,58–60] indicates that the upconversion threshold is much higher for $[Ru(dmb)_3][PF_6]_2$. We attribute the more efficient upconversion of **Pt-5** and **Pt-6** to the long-lived triplet excited states, especially ^{3}IL state of **Pt-6**.

The upconversion is visible with unaided eye (Fig. 12). For $Ru(dmb)_3[PF_6]_2$ and **Pt-3**, orange and red emission were observed, respectively. The emission hardly changed in the presence of DPA, due to the lack of TTA upconversion (Fig. 12). For **Pt-5** and **Pt-6**, however, the emission color changed drastically in the presence of DPA, due to the significant TTA upconversion with the two sensitizers (Fig. 12). The color changes of the solutions were quantified using the CIE coordinates of the emission of the solutions (Fig. 12c and 12d). For example, the emission of **Pt-3** is (0.63, 0.37). In the presence of DPA, the CIE coordinates changed a little to (0.58, 0.34). For **Pt-5** and **Pt-6**, however, significant changes in the CIE coordinates were observed in the presence of DPA. For **Pt-5**, the CIE changed from (0.63, 0.37) to (0.30, 0.14) in the presence of DPA. Similar results were observed for the CIE change of **Pt-6**, for which the CIE coordinates (0.64, 0.36) moved into the deep blue region (0.17, 0.05) in the presence of DPA.

The quenched phosphorescence peak area is much smaller than the observed upconversion peak area (Fig. 11). Thus we propose that dark excited state will also sensitize the TTET. TTET does not required an emissive triplet excited state to initiate the process.

In order to quantitatively study the efficiency of the triplet–triplet energy transfer from the sensitizers to DPA, the quenching effect of DPA on the phosphorescence emission of the complexes was studied (Fig. 13). Based on the quenching constants (Table 5), the TTET between **Pt-6** and DPA ($K_{SV} = 3.95 \times 10^5$ M^{-1}) is 12.5

Table 5 Lifetimes (τ), Stern–Volmer quenching constant (K_{SV}) and bimolecular quenching constants (k_q) of the Pt(II) complexes with ^{3}MLCT excited states and ^{3}IL excited states. In deaerated CH_3CN solution. 25 °C

	τ/μs	Φ_{UC}	$K_{sv}/M^{-1}(\times 10^3)$	$k_q/M^{-1}s^{-1}$ $(\times 10^9)$	r^2
Pt-1	3.5	0.0%	30.6	8.74	0.998
Pt-2	3.1	0.0%	83.1	26.80	0.989
Pt-3	4.4	1.4%	31.5	7.88	0.991
Pt-4	6.1	0.0%	136.4	22.36	0.995
Pt-5	13.4	9.9%	145.7	10.87	0.990
Pt-6	21.0	17.7%	394.7	18.80	0.998
Ru(dmb)$_3$	0.87	0.0%	3.08	3.54	0.975

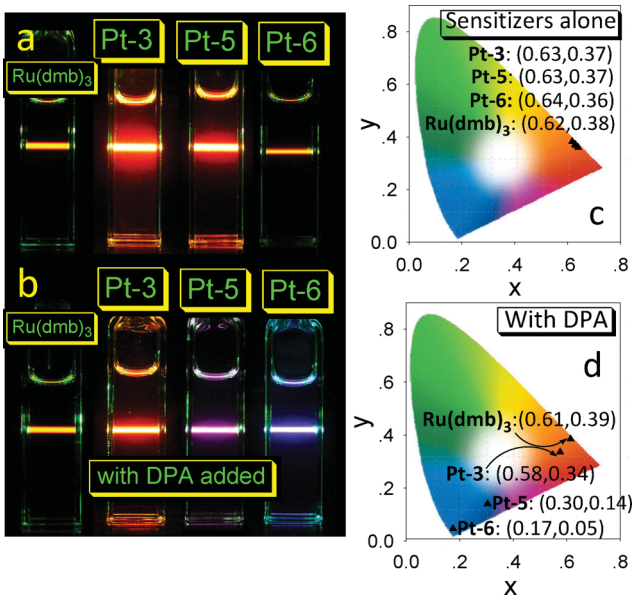

Fig. 12 Photographs of the emission of (a) sensitizers alone and (b) the upconversion. (c) CIE diagram of the emission of sensitizers alone and (d) in the presence of DPA (upconversion). $\lambda_{ex} = 532$ nm (17 mW). In deareated MeCN, *c*[sensitizer] = 2.0×10^{-6} M, *c*[DPA] = 1.1×10^{-5} M. 20 °C.

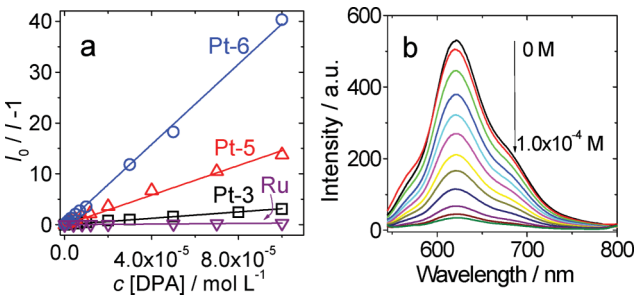

Fig. 13 (a) Stern–Volmer plots generated from the intensity quenching of complexes photoluminescence measured as a function of DPA concentration in CH_3CN. The concentrations of the complexes are 2.0×10^{-6} mol dm^{-3}. λex = 530 nm. (b) Phosphorescence emission spectra of complex **Pt-5** with increasing DPA concentration in deaerated CH_3CN. 20 °C.

times that of **Pt-3** ($K_{SV} = 3.15 \times 10^4$ M^{-1}). Noteably, the Stern–Volmer quenching constant is 128 times that of the triplet sensitizer $[Ru(dmb)_3][PF_6]_2$ ($K_{SV} = 3.08 \times 10^3$ M^{-1}).[59] We attribute this large quenching constant to the long-lived triplet excited state of **Pt-6**. Similar efficient quenching was observed for **Pt-5** ($K_{SV} = 1.46 \times 10^5$ M^{-1}).

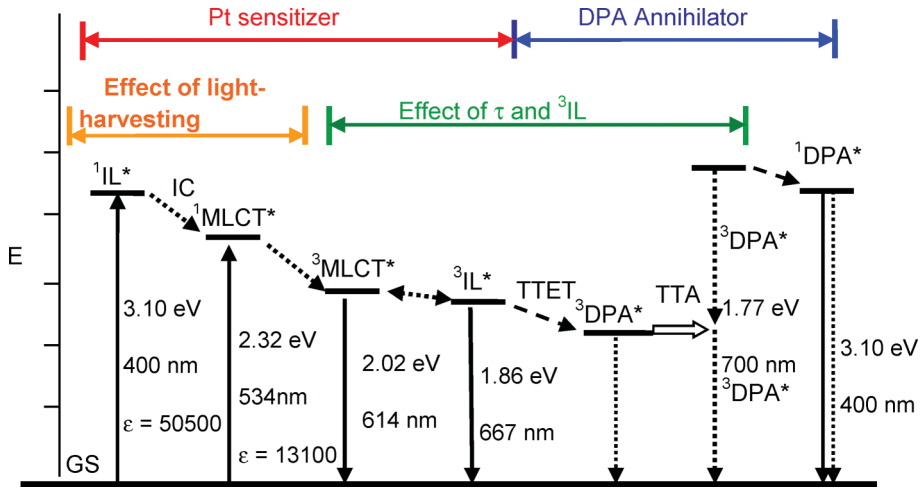

Scheme 2 Jablonski Diagram illustrating the sensitized TTA upconversion process between Schiff base Pt(II) arrays and DPA, exemplified by **Pt-6**. The effect of the light-harvesting ability and the phosphorescence lifetimes of the Pt(II) sensitizers on the efficiency of TTA upconversion is also shown (please note that the vibration energy levels of each electronic state are omitted for clarity). *E* is energy. GS is ground state (S_0). ^{1}IL* is intraligand singlet excited state (pyrene localized). IC is inner conversion. ^{1}MLCT* is the Pt(II) based metal-to-ligand charge transfer singlet excited state. ISC is intersystem crossing. ^{3}MLCT* is the Pt(II) based metal-to-ligand-charge-transfer triplet excited state. ^{3}IL* is intraligand triplet excited state (pyrene localized). We propose that the ^{3}IL* and ^{3}MLCT* of **Pt-5** and **Pt-6** is in equilibrium, but the ^{3}IL feature is more significant for the T_1 state of **Pt-6**. TTET is triplet–triplet energy transfer. ^{3}DPA* is the triplet excited state of DPA. TTA is triplet–triplet annihilation. ^{1}DPA* is the singlet excited state of DPA. The emission bands observed in the TTA experiment are the simultaneous ^{3}MLCT* emission (phosphorescence) and ^{1}DPA* emission (fluorescence). The typical power density of the laser used in the upconversion is 240 mW cm^{-2}, too low to observe simultaneous two-photon absorption.

Thus our results demonstrated the potential for tuning the triplet excited states of Pt(II) Schiff base complexes and the application of the new materials for triplet–triplet-energy tranfer, *e.g.* for luminescent O_2 sensing and triplet–triplet-annihilation based upconversion.

The effect of the intense absorption and long-lived triplet excited states of the Pt(II) Schiff base complexes, especially **Pt-5** and **Pt-6**, on the TTA upconversion, as well as the photophysics of TTA upconversion, are summarized in Scheme 2. Intense absorption is a prerequisite for efficient TTA upconversion, for which more T_1 states of the sensitizers can be populated with photoexcitation. The crucial step for TTA upconversion is the TTET between the triplet sensitizer and the triplet acceptor (DPA), this energy transfer process can be enhanced by the long lifetime of the triplet excited state of the sensitizer. As we have demonstrated that the lifetime of T_1 states of **Pt-5** and **Pt-6** are much longer than those of the model complexes, thus significant TTA upconversion can be expected for **Pt-5** and **Pt-6** compared to other Pt(II) Schiff base complexes described herein.

Conclusions

We have synthesized new Pt(II) Schiff base complexes containing pyrene or ethynylated pyrene subunits by using the *chemistry-on-complex* approach. The complexes show intense absorption in the visible region ($\varepsilon = 1.31 \times 10^4$ M^{-1} cm^{-1} at 530 nm) and room temperature phosphorescence (550–670 nm). The complexes show much longer phosphorescence lifetimes (τ = 21.0 μs) than the model complex (τ = 4.4 μs). The extension of the triplet excited state lifetimes are attributed to the perturbation of the ^{3}MLCT (coordination core localized) by the ^{3}IL state (pyrene localized). For the complexes with ethynylated pyrene subunit, we propose that the phosphorescence is due to the long-lived ^{3}IL excited state. For the complex with C–C linkage between the pyrene and the Schiff base ligand, an equilibrium between the ^{3}MLCT and ^{3}IL state is proposed. These assignments are supported by steady state and nanosecond time-resolved spectra, emission spectra at 77 K and DFT calculations. The visible-light harvesting and the long-lived triplet excited states of the pyrene containing complexes were employed for triplet–triplet-energy-tranfer, *i.e.* luminescent O_2 sensing and triplet–triplet annihilation (TTA) based upconversion. The O_2 sensitivity (Stern–Volmer quenching constant) of the complexes was quantitatively evaluated with polymer films. The results show that the O_2 sensitivity of the pyrene containing complex is 9.0 times that of the model complex **Pt-3** and 13.0 times that of a recently reported cyclometallated Ir(III) complex. Furthermore, significant upconversion (upconversion quantum yield Φ_{UC} = 17.7%) were observed with the pyrene containing complexes as the triplet sensitizers for the TTA based upconversion. Our approach to tune the triplet excited states of the Pt(II) Schiff base complexes with organic chromophores that show appropriate energy levels and the application of the long-lived triplet excited states of the dyads will be useful for design of phosphorescent transition metal complexes and their applications in upconversion, luminescent O_2 sensing, photovoltaics, photo-induced charge seperation, *etc.*

Acknowledgements

We thank the NSFC (20972024 and 21073028), the Fundamental Research Funds for the Central Universities (DUT10ZD212 and DUT11LK19), Ministry of Education (SRFDP-200801410004

and NCET-08-0077), the Royal Society (UK) and NSFC (China-UK Cost-Share Science Networks, 21011130154), State Key Laboratory of Fine Chemicals (KF0802), State Key Laboratory of Chemo/Biosensing and Chemometrics (2008009), Education Department of Liaoning Province (2009T015) for financial support.

Notes and references

1 J. A. G. Williams, *Top. Curr. Chem.*, 2007, **281**, 205.
2 (*a*) L. Flamigni, A. Barbieri, C. Sabatini, B. Ventura and F. Barigelletti, *Top. Curr. Chem.*, 2007, **281**, 143; (*b*) S. Develay and J. A. Gareth Williams, *Dalton Trans.*, 2008, 4562–4564; (*c*) P.-H. Lanoë, H. L. Bozec, J. A. Gareth Williams, J.-L. Fillaut and V. Guerchais, *Dalton Trans.*, 2010, **39**, 707.
3 S. Ji, H. Guo, X. Yuan, X. Li, H. Ding, P. Gao, C. Zhao, W. Wu, W. Wu and J. Zhao, *Org. Lett.*, 2010, **12**, 2876.
4 W. Wu, W. Wu, S. Ji, H. Guo, P. Song, K. Han, L. Chi, J. Shao and J. Zhao, *J. Mater. Chem.*, 2010, **20**, 9775.
5 W. Wu, W. Wu, S. Ji, H. Guo and J. Zhao, *Dalton Trans.*, 2011, **40**, 5953–5963.
6 H. Sun, H. Guo, W. Wu, X. Liu and J. Zhao, *Dalton Trans.*, 2011, **40**, 7834–7841.
7 (*a*) N. Chawdhury, A. Köhler, R. H. Friend, W.-Y. Wong, J. Lewis, M. Younus, P. R. Raithby, T. C. Corcoran, M. R. A. Al-Mandhary and M. S. Khan, *J. Chem. Phys.*, 1999, **110**, 4963; (*b*) J. Ni, L.-Y. Zhang, H.-M. Wen and Z.-N. Chen, *Chem. Commun.*, 2009, 3801.
8 W.-Y. Wong, *Dalton Trans.*, 2007, **36**, 4495.
9 W.-Y. Wong and C.-L. Ho, *Coord. Chem. Rev.*, 2006, **250**, 2627.
10 W.-Y. Wong and C.-L. Ho, *Coord. Chem. Rev.*, 2009, **253**, 1709.
11 W.-Y. Wong and C.-L. Ho, *J. Mater. Chem.*, 2009, **19**, 4457.
12 G.-J. Zhou and W.-Y. Wong, *Chem. Soc. Rev.*, 2011, **40**, 2541.
13 G.-J. Zhou, W.-Y. Wong, Z. Lin and C. Ye, *Angew. Chem., Int. Ed.*, 2006, **45**, 6189.
14 G. Zhou, W.-Y. Wong, S.-Y. Poon, C. Ye and Z. Lin, *Adv. Funct. Mater.*, 2009, **19**, 531.
15 M. Hissler, A. Harriman, A. Khatyr and R. Ziessel, *Chem.–Eur. J.*, 1999, **5**, 3366.
16 P.-H. Lanoë, J.-L. Fillaut, L. Toupet, J. A. G. Williams, H. Le Bozeca and V. Guerchais, *Chem. Commun.*, 2008, 4333.
17 G.-J. Zhou, Q. Wang, W.-Y. Wong, D. Ma, L. Wang and Z. Lin, *J. Mater. Chem.*, 2009, **19**, 1872.
18 Z. He, W.-Y. Wong, X. Yu, H.-S. Kwok and Z. Lin, *Inorg. Chem.*, 2006, **45**, 10922.
19 B. Yin, F. Niemeyer, J. A. G. Williams, J. Jiang, A. Boucekkine, L. Toupet, H. L. Bozec and V. Guerchais, *Inorg. Chem.*, 2006, **45**, 8584.
20 W.-Y. Wong and C.-L. Ho, *Acc. Chem. Res.*, 2010, **43**, 1246.
21 D. N. Kozhevnikov, V. N. Kozhevnikov, M. Z. Shafikov, A. M. Prokhorov, D. W. Bruce and J. A. G. Williams, *Inorg. Chem.*, 2011, **50**, 3804.
22 I. V. Sazanovich, M. A. H. Alamiry, J. Best, R. D. Bennett, O. V. Bouganov, E. S. Davies, V. P. Grivin, A. J. H. M. Meijer, V. F. Plyusnin, K. L. Ronayne, A. H. Shelton, S. A. Tikhomirov, M. Towrie and J. A. Weinstein, *Inorg. Chem.*, 2008, **47**, 10432.
23 F. N. Castellano, I. E. Pomestchenko, E. Shikhova, F. Hua, M. L. Muro and N. Rajapakse, *Coord. Chem. Rev.*, 2006, **250**, 1819.
24 C. Ed Whittle, J. A. Weinstein, M. W. George and K. S. Schanze, *Inorg. Chem.*, 2001, **40**, 4053.
25 M. Hissler, W. B. Connick, D. K. Geiger, J. E. McGarrah, D. Lipa, R. J. Lachicotte and R. Eisenberg, *Inorg. Chem.*, 2000, **39**, 447.
26 X. Han, L. Z. Wu, G. Si, J. Pan, Q.-Z. Yang, L.-P. Zhang and C.-H. Tung, *Chem.–Eur. J.*, 2007, **13**, 1231.
27 H. Guo, M. L. Muro-Small, S. Ji, J. Zhao and F. N. Castellano, *Inorg. Chem.*, 2010, **49**, 6802.
28 (*a*) S. Ji, W. Wu, W. Wu, H. Guo and J. Zhao, *Angew. Chem., Int. Ed.*, 2011, **50**, 1626; (*b*) S. Ji, H. Guo, W. Wu, W. Wu and J. Zhao, *Angew. Chem., Int. Ed.*, 2011, **50**, 8283.
29 Y. Liu, W. Wu, X. Zhang, H. Guo and J. Zhao, *Dalton Trans.*, 2011, **40**, 9085.
30 J. I. Goldsmith, W. R. Hudson, M. S. Lowry, T. H. Anderson and S. Bernhard, *J. Am. Chem. Soc.*, 2005, **127**, 7502.
31 (*a*) X. Wang, S. Goeb, Z. Ji, N. A. Pogulaichenko and F. N. Castellano, *Inorg. Chem.*, 2011, **50**, 705; (*b*) A. A. Rachford, R. Ziessel, T. Bura, P. Retailleau and F. N. Castellano, *Inorg. Chem.*, 2010, **49**, 3730; (*c*) M. Galletta, S. Campagna, M. Quesada, G. Ulrich and R. Ziessel, *Chem. Commun.*, 2005, 4222.
32 (*a*) C.-M. Che, C.-C. Kwok, S.-W. Lai, A. F. Rausch, W. J. Finkenzeller, N. Zhu and H. Yersin, *Chem.–Eur. J.*, 2010, **16**, 233; (*b*) Z. Guo, W.-L. Tong and M. C. W. Chan, *Chem. Commun.*, 2009, 6189.
33 L. Xiong, Q. Zhao, H. Chen, Y. Wu, Z. Dong, Z. Zhou and F. Li, *Inorg. Chem.*, 2010, **49**, 6402.
34 J. Brooks, Y. Babayan, S. Lamansky, P. I. Djurovich, I. Tsyba, R. Bau and M. E. Thompson, *Inorg. Chem.*, 2002, **41**, 3055.
35 G.-J. Zhou, W.-Y. Wong, B. Yao, Z. Xie and L. Wang, *J. Mater. Chem.*, 2008, **18**, 1799.
36 S. Ji, W. Wu, W. Wu, P. Song, K. Han, Z. Wang, S. Liu, H. Guo and J. Zhao, *J. Mater. Chem.*, 2010, **20**, 1953.
37 H. Guo, S. Ji, W. Wu, W. Wu, J. Shao and J. Zhao, *Analyst*, 2010, **135**, 2832.
38 X. Wang, A. D. Guerzo and R. H. Schmehl, *J. Photochem. Photobiol., C*, 2004, **5**, 55.
39 N. D. McClenaghan, Y. Leydet, B. Maubert, M. T. Indelli and S. Campagnab, *Coord. Chem. Rev.*, 2005, **249**, 1336.
40 A. I. Baba, J. R. Shaw, J. A. Simon, R. P. Thummel and R. H. Schmehl, *Coord. Chem. Rev.*, 1998, **171**, 43.
41 W. Wu, S. Ji, W. Wu, H. Guo, X. Wang, J. Zhao and Z. Wang, *Sens. Actuators, B*, 2010, **149**, 395.
42 M. J. Frisch, G. W. Trucks, H. B. Schlegel, G. E. Scuseria, M. A. Robb, J. R. Cheeseman, G. Scalmani, V. Barone, B. Mennucci, G. A. Petersson, H. Nakatsuji, M. Caricato, X. Li, H. P. Hratchian, A. F. Izmaylov, J. Bloino, G. Zheng, J. L. Sonnenberg, M. Hada, M. Ehara, K. Toyota, R. Fukuda, J. Hasegawa, M. Ishida, T. Nakajima, Y. Honda, O. Kitao, H. Nakai, T. Vreven, J. A. Montgomery, Jr., J. E. Peralta, F. Ogliaro, M. Bearpark, J. J. Heyd, E. Brothers, K. N. Kudin, V. N. Staroverov, R. Kobayashi, J. Normand, K. Raghavachari, A. Rendell, J. C. Burant, S. S. Iyengar, J. Tomasi, M. Cossi, N. Rega, J. M. Millam, M. Klene, J. E. Knox, J. B. Cross, V. Bakken, C. Adamo, J. Jaramillo, R. Gomperts, R. E. Stratmann, O. Yazyev, A. J. Austin, R. Cammi, C. Pomelli, J. Ochterski, R. L. Martin, K. Morokuma, V. G. Zakrzewski, G. A. Voth, P. Salvador, J. J. Dannenberg, S. Dapprich, A. D. Daniels, O. Farkas, J. B. Foresman, J. V. Ortiz, J. Cioslowski and D. J. Fox, *GAUSSIAN 09 (Revision A.1)*, Gaussian, Inc., Wallingford, CT, 2009.
43 T. N. Singh-Rachford and F. N. Castellano, *Coord. Chem. Rev.*, 2010, **254**, 2560.
44 I. E. Pomestchenko and F. N. Castellano, *J. Phys. Chem. A*, 2004, **108**, 3485.
45 D. N. Kozhevnikov, V. N. Kozhevnikov, M. M. Ustinova, A. Santoro, D. W. Bruce, B. Koenig, R. Czerwieniec, T. Fischer, M. Zabel and H. Yersin, *Inorg. Chem.*, 2009, **48**, 4179.
46 X. Zhang, L. Chi, S. Ji, Y. Wu, P. Song, K. Han, H. Guo, T. D. James and J. Zhao, *J. Am. Chem. Soc.*, 2009, **131**, 17452.
47 S. Ji, J. Yang, Q. Yang, S. Liu, M. Chen and J. Zhao, *J. Org. Chem.*, 2009, **74**, 4855.
48 T. Kowalczyk, Z. Lin and T. V. Voorhis, *J. Phys. Chem. A*, 2010, **114**, 10427.
49 X. Zhang, Y. Wu, S. Ji, H. Guo, P. Song, K. Han, W. Wu, W. Wu, T. D. James and J. Zhao, *J. Org. Chem.*, 2010, **75**, 2578.
50 J. R. Lakowicz, *Principles of Fluorescence Spectroscopy*, 2nd ed., Kluwer Academic/Plenum Publishers, New York, 1999.
51 B. Valeur, *Molecular Fluorescence: Principles and Applications*, Wiley-VCH, Verlag GmbH, New York, 2001.
52 S. Ji, W. Wu, Y. Wu, T. Zhao, F. Zhou, Y. Yang, X. Zhang, X. Liang, W. Wu, L. Chi, Z. Wang and J. Zhao, *Analyst*, 2009, **134**, 958.
53 W. Wu, W. Wu, S. Ji, H. Guo and J. Zhao, *J. Organomet. Chem.*, 2011, **696**, 2388.
54 W. Wu, C. Cheng, W. Wu, H. Guo, S. Ji, P. Song, K. Han, J. Zhao, X. Zhang, Y. Wu and G. Du, *Eur. J. Inorg. Chem.*, 2010, **29**, 4683.
55 W. Wu, W. Wu, S. Ji, H. Guo and J. Zhao, *Eur. J. Inorg. Chem.*, 2010, **29**, 4470.
56 S. M. Borisov and I. Klimant, *Anal. Chem.*, 2007, **79**, 7501.
57 C. S. K. Mak, D. Pentlehner, M. Stich, O. S. Wolfbeis, W. K. Chan and H. Yersin, *Chem. Mater.*, 2009, **21**, 2173.
58 D. V. Kozlov and F. N. Castellano, *Chem. Commun.*, 2004, 2860.
59 R. R. Islangulov, D. V. Kozlov and F. N. Castellano, *Chem. Commun.*, 2005, 3776.
60 P. Du and R. Eisenberg, *Chem. Sci.*, 2010, **1**, 502.
61 S. Baluschev, V. Yakutkin, T. Miteva, Y. Avlasevich, S. Chernov, S. Aleshchenkov, G. Nelles, A. Cheprakov, A. Yasuda,

K. Müllen and G. Wegner, *Angew. Chem., Int. Ed.*, 2007, **46**, 7693.
62 H.-C. Chen, C.-Y. Hung, K.-H. Wang, H.-L. Chen, W. S. Fann, F.-C. Chien, P. Chen, T. J. Chow, C.-P. Hsu and S.-S. Sun, *Chem. Commun.*, 2009, 4064.
63 Y. Y. Cheng, T. Khoury, R. G. C. R. Clady, M. J. Y. Tayebjee, N. J. Ekins-Daukes, M. J. Crossleya and T. W. Schmidt, *Phys. Chem. Chem. Phys.*, 2010, **12**, 66.
64 A. Monguzzi, J. Mezyk, F. Scotognella, R. Tubino and F. Meinardi, *Phys. Rev. B: Condens. Matter Mater. Phys.*, 2008, **78**, 195112–1.
65 (*a*) A. Monguzzi, R. Tubino and F. Meinardi, *Phys. Rev. B: Condens. Matter Mater. Phys.*, 2008, **77**, 155122–1; (*b*) J. Sun, W. Wu, H. Guo and J. Zhao, *Eur. J. Inorg. Chem.*, 2011, 3165–3173; (*c*) L. Huang, L. Zeng, H. Guo, W. Wu, W. Wu, S. Ji and J. Zhao, *Eur. J. Inorg. Chem.*, 2011, DOI: 10.1002/ejic.201100777.